Published in final edited form as:
J Periodontol. 2014 January ; 85(1): 195–203. doi:10.1902/jop.2013.120651.

Characterization of Periodontal Structures of *Enamelin*-Null Mice

Hsun-Liang Chan[*,†], **William V. Giannobile**[*,‡], **Robert M. Eber**[*], **James P. Simmer**[†], and **Jan C. Hu**[†]

[*]Department of Periodontics and Oral Medicine, University of Michigan School of Dentistry, Ann Arbor, MI

[†]Department of Biologic and Materials Sciences, University of Michigan School of Dentistry

[‡]Department of Biomedical Engineering, University of Michigan College of Engineering, Ann Arbor, MI

Abstract

Background—*Enamelin*-null (*ENAM*$^{-/-}$) mice have no enamel. When characterizing *ENAM*$^{-/-}$ mice, alveolar bone height reduction was observed, and it was hypothesized that enamel defects combined with diet are associated with the periodontal changes of *ENAM*$^{-/-}$ mice. The aim of the present study is to compare the dimension of interradicular bone of *ENAM*$^{-/-}$ (knock-out [KO]) with wild-type (WT) mice, maintained on hard (HC) or soft (SC) chow.

Methods—A total of 100 animals divided into four groups were studied at 3, 8, and 24 weeks of age: 1) KO/HC; 2) KO/SC; 3) WT/HC; and 4) WT/SC. Microcomputed tomography was performed, and the following measurements were made between mandibular first (M1) and second (M2) molars: relative alveolar bone height (RBH), crestal bone width (CBW), bone volume (BV), bone mineral content (BMC), and bone mineral density (BMD). The position of M1 and M2 in relation to the inferior border of the mandible was also determined at 24 weeks. All variables were analyzed by one-way analysis of variance and Dunnett test for pairwise comparisons. Morphologic analyses were conducted on hematoxylin and eosin–stained sections.

Results—Radiographically, the enamel layer was absent in *ENAM*$^{-/-}$ mice. Interproximal open contacts were observed exclusively in *ENAM*$^{-/-}$ mice, and the prevalence decreased over time, suggesting that a shifting of tooth position had occurred. Additionally, in the two *ENAM*$^{-/-}$ groups, RBH was significantly lower at 8 and 24 weeks (P <0.02); CBW, BV, and BMC were significantly less (P <0.05) at 24 weeks. No differences in BMD were found among the four groups. The molars migrated to a more coronal position in *ENAM*$^{-/-}$ mice and mice on HC. Histologic findings were consistent with radiographic observations. After eruption, the junctional epithelium was less organized in *ENAM*$^{-/-}$ mice.

Conclusion—The interdental bone density was not affected in the absence of enamelin, but its volume was, which is likely a consequence of alternations in tooth position.

Correspondence: Dr. Hsun-Liang Chan, Department of Periodontics and Oral Medicine, University of Michigan School of Dentistry, 1011 North University Ave., Ann Arbor, MI 48109. hlchan@umich.edu.

The authors report no conflicts of interest related to this study.

Keywords

Amelogenesis imperfecta; dental enamel; dental enamel proteins; periodontium; x-ray microtomography

Enamelin is the largest enamel matrix protein, and its cleavage products cumulate to make up 5% of the enamel matrix. Defects in human enamelin (*ENAM*, 4q13.2) cause autosomal-dominant amelogenesis imperfecta (AI). To date, 16 *ENAM* mutations are associated with autosomal-dominant AI.[1–16] In general, the clinical features include thin enamel with either severe or localized hypoplasia.[6] The enamel phenotype is dose dependent and ranges from small, well-circumscribed enamel pits to enamel agenesis.[12] Mutations induced with the mutagen *N*-ethyl-*N*-nitrosourea resulted in four separate *ENAM* point mutations: 1) p.S55I; 2) p.E57G; 3) the splice donor site in exon 4; and 4) p.Q176X.[17,18] Heterozygous mice exhibited rough and pitted enamel, whereas the null mice showed enamel agenesis. *Enamelin* gene knock-out (KO) and LacZ knock-in mice were generated by replacing the *ENAM* coding sequence from the translation initiation site through exon 7 with a *lacZ* reporter gene.[19] The enamel layer is completely absent in *enamelin*-null ($ENAM^{-/-}$) mice compared with the mild enamel phenotype in the heterozygotes ($ENAM^{+/-}$). A thin, highly irregular, easily abraded mineralized crust over the dentin is observed in $ENAM^{-/-}$ mice. The affected teeth have significant wear and are generally chalky white. The histologic, morphometric, and protein/mineral analyses demonstrate that enamelin is essential for proper enamel matrix organization and mineralization.

Enamelin, like other enamel matrix proteins, is strictly expressed by ameloblasts during the secretory stage of amelogenesis;[19] as a result, it is unlikely that the absence of enamelin will have a direct effect on periodontium. Interestingly, during the assessment of the body weight of $Enam^{-/-}$ mice, it was observed that the level of alveolar bone seemed decreased, which was also influenced by food texture. From the characterization of $ENAM^{-/-}$ mice,[20] differences in their periodontia compared with wildtype (WT) mice were noticed. Periodontal changes around the mandibular molars, with appreciable bone loss, widened interdental spaces, and furcation involvement in the first molars (M1) and sometimes second molars (M2) were observed among the $ENAM^{-/-}$ mice. This study is designed to compare the dimension of interradicular bone between mandibular M1 and M2 of $ENAM^{-/-}$ KO and WT mice, maintained on hard (HC) or soft (SC) chow. In addition, assessment was made to determine whether there were additional periodontal changes among the KO mice.

MATERIALS AND METHODS

Animal Protocol

All procedures involving animals were reviewed and approved by the institutional animal care and use committee at the University of Michigan (protocol no. 08512). This study conformed to the ARRIVE (Animal research: Reporting of in vivo experiments) guidelines[21] for the conduct of preclinical research.

Experimental Design

The *ENAM*$^{-/-}$ (in C57BL/6 genomic background) and WT C57BL/6 mice were maintained separately on SC or HC[§] throughout the experiment. SC was water-moistened HC. Thus, nutrition facts between the two food types were the same. Four experimental groups were established: 1) WT/HC; 2) WT/SC; 3) *ENAM*$^{-/-}$ HC (knock-out [KO]/HC); and 4) *ENAM*$^{-/-}$ SC (KO/SC). At 3 weeks (n = 10, 10, 10, and 9 for the four groups), 8 weeks (n = 8, 8, 10, and 9), and 24 weeks (n = 5, 6, 6, and 9) after birth, mice were sacrificed by inhalation anesthesia and perfused with ice-cold 4% paraformaldehyde.[‖] Mandibles were carefully dissected and fixed in 4% paraformaldehyde for 24 hours, rinsed with phosphate-buffered saline, and then stored in 70% ethanol[¶] until used.

Microcomputed Tomography Analyses

One of the two hemimandible block biopsies from each mouse was chosen randomly to be scanned by microcomputed tomography (micro-CT).[#] In brief, the x-ray generator was operated at an accelerated potential of 80 kV with a current of 80 μA at 1,100 milliseconds. The resulting images had a voxel size of 18 × 18 × 18 μm^3. Bone mineral density (BMD) per unit (milligrams per cubic centimeters) was calculated and determined with an internal reference programmed in the micro-CT. The software[**] was used for visualization and quantification of two-dimensional (2-D) and three-dimensional (3-D) data in a personal computer. All measurements were made by one examiner (H-LC). Ten percent of the measurements were repeated after 7 days, and intraexaminer agreement was calculated to be 0.88.

Linear Measurements of Alveolar Bone

Because the observed alveolar bone loss in null mice was between M1 and M2 and the morphology of the size of the third molar was variable, the sagittal plane containing the center of the distal root of mandibular M1 (DRM1) and mesial root of mandibular M2 (MRM2) was selected for measurements. The alveolar bone height was presented as a percentage of the root length attributable to a lack of discernible cemento-enamel junction (CEJ) in KO groups. The linear measurements are demonstrated in Figure 1A. The distal root length of M1 (RLM1) and mesial root length of M2 (RLM2) in millimeters were measured with a built-in digital caliber from the furcation fornix (FF) to the root apex. The interproximal bone height between M1 and M2 (BHM1) in millimeters was measured from alveolar crest to the root apex of DRM1 and MRM2, respectively. The relative bone height at M1 (RBHM1) was equated as (BHM1/RLM1) × 100%, and the same was applied to calculate the relative bone height at M2 (RBHM2). The interproximal crestal bone width (CBW) between M1 and M2 was also determined at the level of 100 μm apical to the crest (Fig. 1B).

[§]LabDiet 5001, Purina Mills, St. Louis, MO.
[‖]Thermo Fisher Scientific, Waltham, MA.
[¶]Thermo Fisher Scientific.
[#]mCT 100, Scanco, Wayne, PA.
[**]eXplore MicroView v.2.0, Analysis Plus, GE Healthcare, Waukesha, WI.

To highlight the influence of altered tooth contacts on the interdental bone level of null mice, the volume of alveolar bone at the mesial side of M1, in which there were no tooth contacts, was measured and compared among the 24-week-old experimental groups.

Volumetric Measurements of Alveolar Bone

Before volumetric measurements were made, the orientation of images was determined carefully to ensure reproducibility and comparability when assessing and quantifying alveolar bone. The methods were modified based on Park et al.[22] Briefly, images were positioned using FFs of M1 and M2 as reference points. The FFs of M1 and M2 were chosen because the level of the alveolar bone crest between M1 and M2 was usually coincident with the level at which the two FFs were connected in normal mice. As described, an axial plane was set passing through the two FFs, and the sagittal plane was chosen crossing the center of DRM1 and MRM2. After the reorientation, the selection of a 2-D region of interest (ROI) followed (Fig. 1C). Outlining the ROI started at the axial section in which the two FFs were included and ended at the section of the apex of MRM2. The ROI at each section was bordered by the peripheries of roots (DRM1 and MRM2) mesiodistally and the tangent lines linking the two roots bucco-lingually. The interval of each plane was determined by the anatomic variability; greater dissimilarity between sections required contours to be drawn at smaller plane intervals. The 3-D ROI was constructed based on the 2-D ROIs (Fig. 1D). The following volumetric alveolar bone parameters were calculated: 1) total volume (TV); 2) bone volume (BV); 3) bone volume fraction; 4) bone mineral content (BMC); and 5) BMD.

Tooth Eruption Measurements

Four vertical distances were measured on each 24-week-old mouse sample: from the fornix (F1) and the apex (A1) of distal root of the mandibular M1 (F1M, A1M) as well as the fornix (F2) and the apex (A2) of MRM2 (F2M, A2M) to the pogonion–gnathion plane (Pg–Gn plane) (Fig. 1E). Pg is a point on the most inferior contour of the lower border of the mandible and is adjacent to the incisor, whereas Gn is a point on the most inferior contour of the angular process of the mandible. The measurements were made using the following steps. First, the two anatomically reproducible points, Pg and Gn, were identified to define the axial plane (Pg–Gn plane [red line] in Fig. 1E) that included both points. Second, a sagittal plane that passed through F1, F2, A1, and A2 and was perpendicular to the Pg–Gn plane was constructed. Third, on that sagittal plane, the four linear measurements were made.

Histologic and Immunohistologic Analyses

The other hemimandible that was not used for micro-CT scanning from each mouse was processed for histologic evaluation. The specimens were embedded in paraffin after dehydration with increasing concentration of ethanol (70%, 95%, and 100%) for 1 hour each with one change at 30 minutes. At embedding, the specimens were positioned with the long axis of molars parallel to the horizontal plane. Samples were sectioned mesio-distally at 6 μm using a rotary microtome and then stained with hematoxylin and eosin (H&E) and the tartrate-resistant acid phosphatase (TRAP) stains. The midsagittal sections were chosen for evaluation under the microscope[††] and photographed.[‡‡] The presence of food or foreign

body impaction, the integrity of the periodontal apparatus, the presence of inflammatory cells, the level of the junctional epithelium (JE), alveolar bone, and root surfaces were evaluated and recorded.

Statistical Analyses

Descriptive evaluation of all variables was recorded as mean ± SD. Statistically significant differences of all variables among groups were determined by two-way analysis of variance and Dunnett test for pairwise group comparisons. The association between RBHM1 and CBW was determined with Pearson correlation test. All statistical analyses were conducted with a software package.[§§]

RESULTS

Linear Measurements of Alveolar Bone

The results of linear measurements at three different time points for the four groups are summarized in Figure 2. The root length increased with time, especially between 3 and 8 weeks. The mean value of RLM1 and RLM2 was not significantly different among the four groups at 3, 8, and 24 weeks, suggesting that the root development was not affected by the absence of enamelin (Figs. 2A and 2B). Mean RBHM1 and RBHM2 of KO/HC and KO/SC were significantly lower than the two WT groups at 8 and 24 weeks but not at 3 weeks (Figs. 2C and 2D). In addition, narrower CBW was found, starting at 3 weeks in the KO/ HC group, compared with the WT/HC ($P = 0.003$) and the WT/SC ($P = 0.022$) groups (Fig. 2E). CBW of KO/SC decreased significantly compared with the WT groups at 24 weeks (Fig. 2E).

Volumetric Measurements of Alveolar Bone

The mean volumetric measurements of alveolar bone are summarized in Figure 3. The three values (mean TV, BV, and BMC) of KO/HC were significantly lower at 3 weeks than those of the WT groups. At 24 weeks, the three values of the two null groups were significantly smaller than that of the two WT groups. However, the BMD was similar among the four groups, suggesting that the bone density was not affected by the lack of enamelin.

Tooth Eruption Measurements

There was a trend that the distances of F1M and F2M were longer in KO than in WT mice on the same chow (Fig. 4). A similar trend was also observed in HC compared with SC mice of the same genotype. However, the value was only significantly different between WT/HC + KO/HC and WT/SC + KO/HC at M1 and WT/SC + KO/HC, WT/HC + WT/SC, and WT/SC + KO/SC at M2. The difference in mean A1M and A2M among groups follows the same pattern as that of the F1M and F2M; however, the only significant difference was found between WT/SC + KO/HC at A1 and A2 ($P = 0.02$). Compensatory eruption of

[††]Eclipse E600, Nikon, Belmont, CA.
[‡‡]DXM1200, Mager Scientific, Dexter, MI.
[§§]SPSS v.17.0, IBM, Somers, NY.

molars occurred in the absence of enamel and the presence of occlusal attrition exaggerated by dietary HC.

Correlations

RBHM1 was positively correlated with CBW (R^2 = 0.324, 0.28, and 0.663 for 3, 8, and 24 weeks, respectively), suggesting a relationship between the width and height of the alveolar bone between M1 and M2. In addition, there were positive relationships between volumetric and linear measurements. TV was positively correlated with CBW (R^2 = 0.373, 0.164, and 0.736 for 3, 8, and 24 weeks, respectively). BV was positively related to RBHM1 (R^2 = 0.206, 0.469, and 0.761 for 3, 8, and 24 weeks, respectively).

Histologic and Immunohistologic Results

Representative histologic sections of 24-week-old mice at ×10 magnification are shown in Figures 5A through 5D. In the null mice, the enamel scarcely exists. Compared with the WT specimens, the alveolar bone height was much lower in null specimens. In addition, the interdental space was much narrower in the null mice. In the null mice, the interdental papilla was asymmetric, and the JE was disorganized, as a reflection of uneven CEJs between M1 and M2. There was no appreciable sign of inflammation in null mice. A root defect was frequently observed close to the CEJ on the distal root of M1 in null mice. Although observed in the alveolar bone, TRAP-positive stains were not present on the root defects in 3-weekold null mice (Figs. 5E through 5H).

DISCUSSION

Alveolar Bone Loss in Null Mice

A mouse model expressing a truncated form of ameloblastin, another enamel matrix protein, exhibits JE defects.[23] Lower positioned and porous alveolar bone was observed to be associated with *ENAM*$^{-/-}$ null mice,[19] although not quantified. In the present study, relative bone height between M1 and M2 is significantly lower for 8- and 24-week-old null mice. However, at 3 weeks, there was no significant difference in bone level among the four groups, suggesting that the bone loss is an acquired feature but not a developmental defect attributable to the lack of enamelin. In addition, the BMD of both null groups was not significantly different from that of the two WT groups, indicating that the absence of enamelin did not affect bone density. Furthermore, the bone height at the mesial root of M1 in 24-week-old null mice was not significantly different from that of WT mice. These observations are consistent with the evidence that enamelin is primarily expressed in ameloblasts[19,20] and may not be involved in periodontal development. Together, the alveolar bone loss is unlikely to be a direct effect of the absence of enamelin.

The reduced CBW is positively associated with the reduced alveolar bone height that was observed in null mice. The frequencies of detecting an open contact between M1 and M2 decreased with time in null mice (unpublished data, HL Chan, University of Michigan, Ann Arbor, Michigan), suggesting that there was drifting of teeth occurring after molars were in function. With age, the molars came closer, which resulted in the finding that, at 6 months, both null groups had narrower interdental bone width. Distal drifting of teeth in mice (in

contrast to mesial movement in humans) is a physiologic process,[24] and the present results also show that the CBW at 24 weeks was narrower in all four groups compared with that at 8 weeks. The presence of large diastema between molars attributable to the lack of an enamel layer in null mice might have triggered a more rapid drift, resulting in a narrower interradicular space in null mice.

Reduced interradicular space, or root proximity, is considered a contributory factor for periodontal disease. The term *root proximity* was first described in periodontal literature[25] as an inadequate distance, defined as 1 mm, between the roots of adjacent teeth. A human histologic study[26] demonstrated that the width of the interradicular space dictates what type of tissues could present in that space. When the space was >0.5 mm, cancellous bone flanked by bundle bone could be observed. However, from 0.3 to 0.5 mm, cancellous bone was absent, and the adjacent lamina dura seemed fused. Only periodontal ligament fibers without the presence of bone were found when the distance was reduced to <0.3 mm. A recent human longitudinal study[27] suggested that root proximity poses a risk factor for alveolar bone loss. The alveolar bone height and interradicular distances (IRDs) of mandibular anterior teeth in 473 individuals were followed for up to 23 years. The results showed that sites with IRD <0.6 mm were 28% more likely to lose ≥0.5 mm of bone and 56% (95% confidence interval = 11% to 117%) more likely to lose ≥1.0 mm of bone within 10 years. Together, the available evidence indicated that alveolar bone height is related to the interradicular space. In this study, a positive correlation is found between CBW and alveolar bone height. The narrower interradicular space attributable to the lack of enamel and subsequent tooth drifting might have resulted in the observed narrower CBW and lower alveolar bone height in null mice.

It is found that continuous eruption of molars took place in the null mice at a higher rate than that of the WT. Although higher tooth eruption rate might explain the reduced bone height in null mice, the positive association between F1M/A1M as well as between F2M/A2M supported that this continuous eruption was associated with a bodily movement of the molars toward the occlusal plane rather than an increase of root length. The food texture also influenced such movement, with HC resulting in greater eruption, presumably as a consequence of increased occlusal attrition. Continuous tooth supra-eruption without an increase of the accompanying alveolar bone might have resulted in the observed bone loss in null mice. Active tooth drifting (coronally and interproximally) in the KO groups might have contributed to the apparent osteoclastic activity in the alveolar bone, as represented by TRAP stains (Figs. 5E through 5H). Additionally, foreign body impactions between molars cannot be ruled out as a possible reason for the increased osteoclastic activity.

Linear Measurements Were Substantiated by Volumetric Measurements

Volumetric bone measurement provided a more accurate means of comparing alveolar bone changes because the height of the alveolar bone is irregular, and the linear measurements made on a selected plane might have inevitably introduced some errors. The results of the volumetric analysis were in line with the linear measurements. The TV between M1 and M2 was significantly smaller in KO/HC at 3 and 24 weeks. The TV of the two null groups was smaller than that of the two WT groups. The correlation between TV and CBW was

significant (R^2 = 0.373, 0.164, and 0.736 at 3, 8, and 24 weeks, respectively), indicating that the smaller BV in null mice can be explained by the narrower interdental bone width. BV differences among groups followed a similar pattern as TV and can be explained by decreased RBHM1 because a positive correlation was found between BV and RBHM1 (R^2 = 0.206, 0.469, and 0.761 at 3, 8, and 24 weeks, respectively).

Histologic Findings

During histologic examination, a concave defect of the distal root of M1 was frequently observed in null groups. The cervical root defect was found at all three time points, and the defect seemed self-confined without increasing in size over time. In addition, reparative response by cementum deposition was common as the tooth aged. The location of the defect is restricted to the coronal half of the distal root of M1, although its occurrence in other surface areas cannot be ruled out. Root surface resorptive defects were also found in *amelogenin*-null (*AMELX*$^{-/-}$) mice and were reported to be associated with elevated expression of the receptor activator of the nuclear factor-κB ligand, a key regulator of osteoclastogenesis. [28] However, *AMELX*$^{-/-}$ mice root defects were different from those observed in the *ENAM*$^{-/-}$ mice. Multiple defects occurred in both M1 and M2 in the *AMELX*$^{-/-}$ mice. The defects were positively stained with TRAP in 6-month-old and 1-year-old null mice, whereas in the *ENAM*$^{-/-}$ mice, the defect was singular with a specific location devoid of staining for TRAP. Based on the size, location, and TRAP reactivity, the nature of the cervical lesion in the *ENAM*$^{-/-}$ mice is likely different from that of the *AMELX*$^{-/-}$ mice. Histologic analysis of null mice from the time of root initiation to 3 weeks is necessary to provide insights into the etiology of this root surface defect.

CONCLUSIONS

The periodontium of *ENAM*$^{-/-}$ mice maintained with SC and HC were examined compared with WT mice on the same diet. Alveolar bone height and interproximal bone width between mandibular M1 and M2 had significantly decreased in the 6-month-old *ENAM*$^{-/-}$ mice. The decrease of bone height and width is possibly a consequence of the drifting of the teeth toward each other because of the lack of enamel. However, other reasons, such as a greater tooth eruption rate, etc., cannot be ruled out. This preclinical model can be useful in studying the influence of crown morphology on the integrity of periodontal structure. A next step would be to study patients with hypoplastic AI to determine whether differences in their periodontal features are correlated with increased risk for periodontal disease.

Acknowledgments

This study was supported by National Institute of Dental and Craniofacial Research Grant DE011301. The authors thank Dr. Yuanyuan Hu, Research Laboratory Specialist in Dental Research Laboratory, University of Michigan School of Dentistry, Ann Arbor, Michigan, and Dr. Chan-Ho Park, former student at the College of Engineering, University of Michigan, Ann Arbor, Michigan, now a research fellow at the Department of Periodontology, School of Dentistry, Seoul National University, Seoul, South Korea, for their technical consultations and Mr. Chris Strayhorn, Histology Core, University of Michigan School of Dentistry, for his technical assistance.

References

1. Chan HC, Estrella NM, Milkovich RN, Kim JW, Simmer JP, Hu JC. Target gene analyses of 39 amelogenesis imperfecta kindreds. Eur J Oral Sci. 2011; 119(Suppl 1):311–323. [PubMed: 22243262]
2. Chan HC, Mai L, Oikonomopoulou A, et al. Altered enamelin phosphorylation site causes amelogenesis imperfecta. J Dent Res. 2010; 89:695–699. [PubMed: 20439930]
3. Gutierrez SJ, Chaves M, Torres DM, Briceño I. Identification of a novel mutation in the enamalin gene in a family with autosomal-dominant amelogenesis imperfecta. Arch Oral Biol. 2007; 52:503–506. [PubMed: 17316551]
4. Hart PS, Michalec MD, Seow WK, Hart TC, Wright JT. Identification of the enamelin (g. 8344delG) mutation in a new kindred and presentation of a standardized ENAM nomenclature. Arch Oral Biol. 2003; 48:589–596. [PubMed: 12828988]
5. Hart TC, Hart PS, Gorry MC, et al. Novel ENAM mutation responsible for autosomal recessive amelogenesis imperfecta and localised enamel defects. J Med Genet. 2003; 40:900–906. [PubMed: 14684688]
6. Hu JC, Yamakoshi Y. Enamelin and autosomaldominant amelogenesis imperfecta. Crit Rev Oral Biol Med. 2003; 14:387–398. [PubMed: 14656895]
7. Kang HY, Seymen F, Lee SK, et al. Candidate gene strategy reveals ENAM mutations. J Dent Res. 2009; 88:266–269. [PubMed: 19329462]
8. Kida M, Ariga T, Shirakawa T, Oguchi H, Sakiyama Y. Autosomal-dominant hypoplastic form of amelogenesis imperfecta caused by an enamelin gene mutation at the exon-intron boundary. J Dent Res. 2002; 81:738–742. [PubMed: 12407086]
9. Kim JW, Seymen F, Lin BP, et al. ENAM mutations in autosomal-dominant amelogenesis imperfecta. J Dent Res. 2005; 84:278–282. [PubMed: 15723871]
10. Kim JW, Simmer JP, Lin BP, Seymen F, Bartlett JD, Hu JC. Mutational analysis of candidate genes in 24 amelogenesis imperfecta families. Eur J Oral Sci. 2006; 114(Suppl 1):3–12. discussion 39–41, 379. [PubMed: 16674655]
11. Mårdh CK, Bäckman B, Holmgren G, Hu JC, Simmer JP, Forsman-Semb K. A nonsense mutation in the enamelin gene causes local hypoplastic autosomal dominant amelogenesis imperfecta (AIH2). Hum Mol Genet. 2002; 11:1069–1074. [PubMed: 11978766]
12. Ozdemir D, Hart PS, Firatli E, Aren G, Ryu OH, Hart TC. Phenotype of ENAM mutations is dosage-dependent. J Dent Res. 2005; 84:1036–1041. [PubMed: 16246937]
13. Rajpar MH, Harley K, Laing C, Davies RM, Dixon MJ. Mutation of the gene encoding the enamel-specific protein, enamelin, causes autosomal-dominant amelogenesis imperfecta. Hum Mol Genet. 2001; 10:1673–1677. [PubMed: 11487571]
14. Simmer SG, Estrella NM, Milkovich RN, Hu JC. Autosomal dominant amelogenesis imperfecta associated with ENAM frameshift mutation p.Asn36Ilefs56. Clin Genet. 2013; 83:195–197. [PubMed: 22540999]
15. Urzúa OB, Ortega PA, Rodríguez ML, Morales BI. Genetic, clinical and molecular analysis of a family affected by amelogenesis imperfecta (in Spanish). Rev Med Chil. 2005; 133:1331–1340. [PubMed: 16446857]
16. Wright JT, Torain M, Long K, et al. Amelogenesis imperfecta: Genotype-phenotype studies in 71 families. Cells Tissues Organs. 2011; 194:279–283. [PubMed: 21597265]
17. Masuya H, Shimizu K, Sezutsu H, et al. Enamelin (Enam) is essential for amelogenesis: ENU-induced mouse mutants as models for different clinical subtypes of human amelogenesis imperfecta (AI). Hum Mol Genet. 2005; 14:575–583. [PubMed: 15649948]
18. Seedorf H, Klaften M, Eke F, Fuchs H, Seedorf U, Hrabe de Angelis M. A mutation in the enamelin gene in a mouse model. J Dent Res. 2007; 86:764–768. [PubMed: 17652207]
19. Hu Y, Papagerakis P, Ye L, Feng JQ, Simmer JP, Hu JC. Distal cis-regulatory elements are required for tissue-specific expression of enamelin (Enam). Eur J Oral Sci. 2008; 116:113–123. [PubMed: 18353004]
20. Hu JC, Hu Y, Smith CE, et al. Enamel defects and ameloblast-specific expression in Enam knock-out/lacz knock-in mice. J Biol Chem. 2008; 283:10858–10871. [PubMed: 18252720]

21. Kilkenny C, Browne WJ, Cuthill IC, Emerson M, Altman DG. Improving bioscience research reporting: The ARRIVE guidelines for reporting animal research. PLoS Biol. 2010; 8:e1000412. [PubMed: 20613859]
22. Park CH, Abramson ZR, Taba M Jr, et al. Three-dimensional micro-computed tomographic imaging of alveolar bone in experimental bone loss or repair. J Periodontol. 2007; 78:273–281. [PubMed: 17274716]
23. Wazen RM, Moffatt P, Zalzal SF, Yamada Y, Nanci A. A mouse model expressing a truncated form of ameloblastin exhibits dental and junctional epithelium defects. Matrix Biol. 2009; 28:292–303. [PubMed: 19375505]
24. Kimura R, Anan H, Matsumoto A, Noda D, Maeda K. Dental root resorption and repair: Histology and histometry during physiological drift of rat molars. J Periodontal Res. 2003; 38:525–532. [PubMed: 12941078]
25. Trossello VK, Gianelly AA. Orthodontic treatment and periodontal status. J Periodontol. 1979; 50:665–671. [PubMed: 294480]
26. Heins PJ, Wieder SM. A histologic study of the width and nature of inter-radicular spaces in human adult pre-molars and molars. J Dent Res. 1986; 65:948–951. [PubMed: 3458748]
27. Kim T, Miyamoto T, Nunn ME, Garcia RI, Dietrich T. Root proximity as a risk factor for progression of alveolar bone loss: The Veterans Affairs Dental Longitudinal Study. J Periodontol. 2008; 79:654–659. [PubMed: 18380558]
28. Hatakeyama J, Sreenath T, Hatakeyama Y, et al. The receptor activator of nuclear factor-kappa B ligand-mediated osteoclastogenic pathway is elevated in amelogenin-null mice. J Biol Chem. 2003; 278:35743–35748. [PubMed: 12851394]

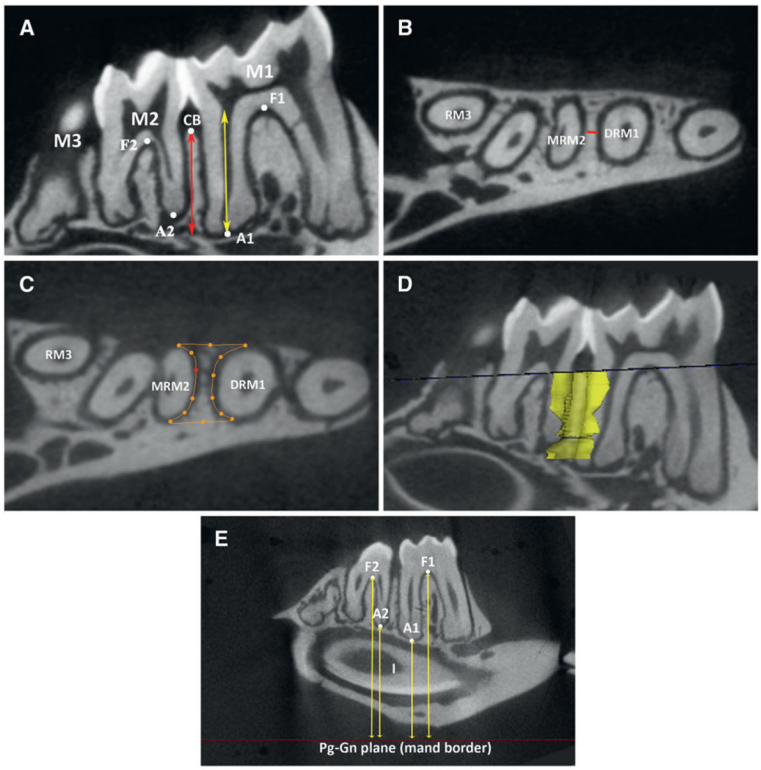

Figure 1.

Illustration of linear measurements. A = apex; CB = crestal bone; F = furcation; RM3 = root of third molar. Root length (yellow arrow) and alveolar bone height (red arrow) of M1**(A)**, CBW between M1 and M2(red line) **(B)**, selection of 2-D ROI (orange outline) **(C)**, and 3-D ROI selection (yellow) **(D). E)** Illustration of the measurements of the furcations (F1, F2) and apices (A1, A2) of the molars in relation to the inferior border of the mandible (Pg–Gn plane, red line). DRM1 = distal root of molar 1; MRM2 = mesial root of molar 2.

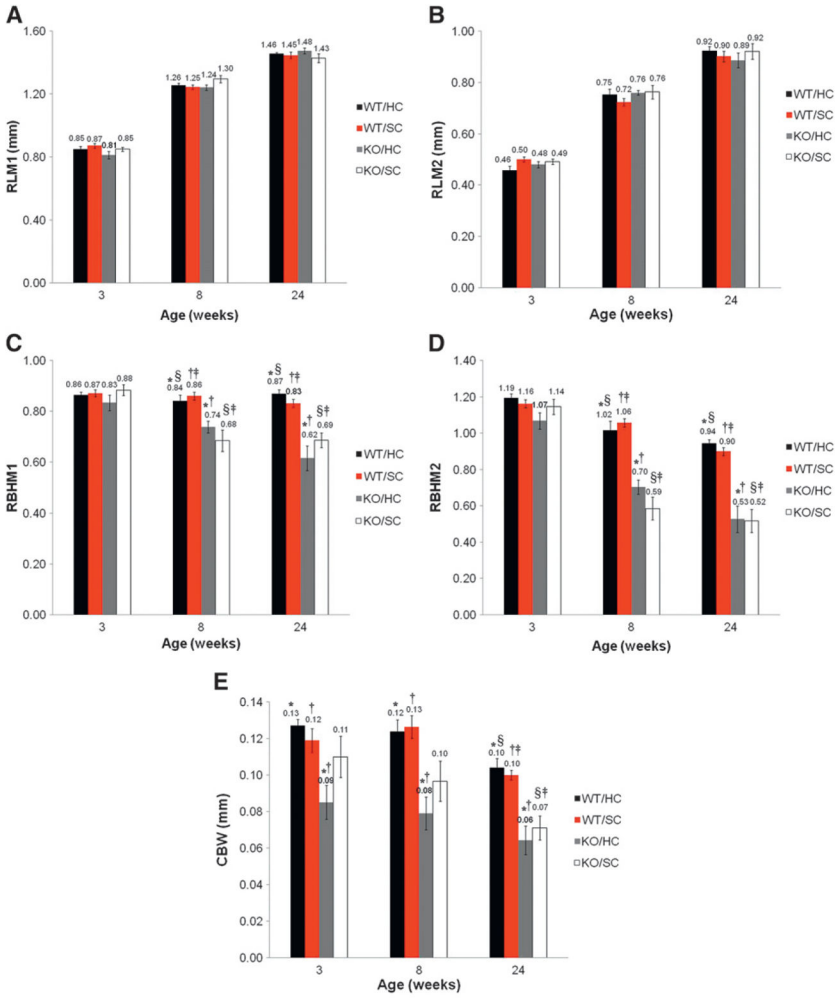

Figure 2.

Comparisons of root length, relative bone height, and CBW at 3, 8, and 24 weeks. RLM1 **(A)**, RLM2 **(B)**, RBHM1 **(C)**, RBHM2 **(D)**, and CBW **(E)**. Groups with the same symbols showed statistically significant differences at the given time point ($P \leq 0.05$).

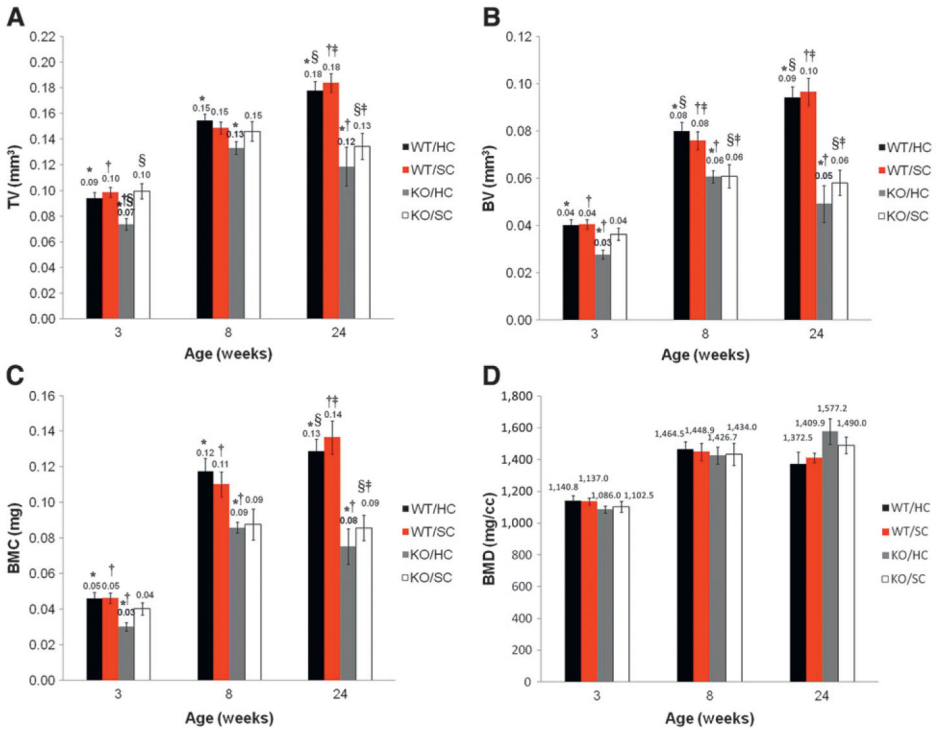

Figure 3.

Comparisons of the volumetric measurements betweenM1 andM2at 3, 8, and 24weeks. TV **(A)**, BV **(B)**, BMC **(C)**, and BMD **(D)**. Groups with the same symbols showed statistically significant differences at the given time point ($P \leq 0.05$).

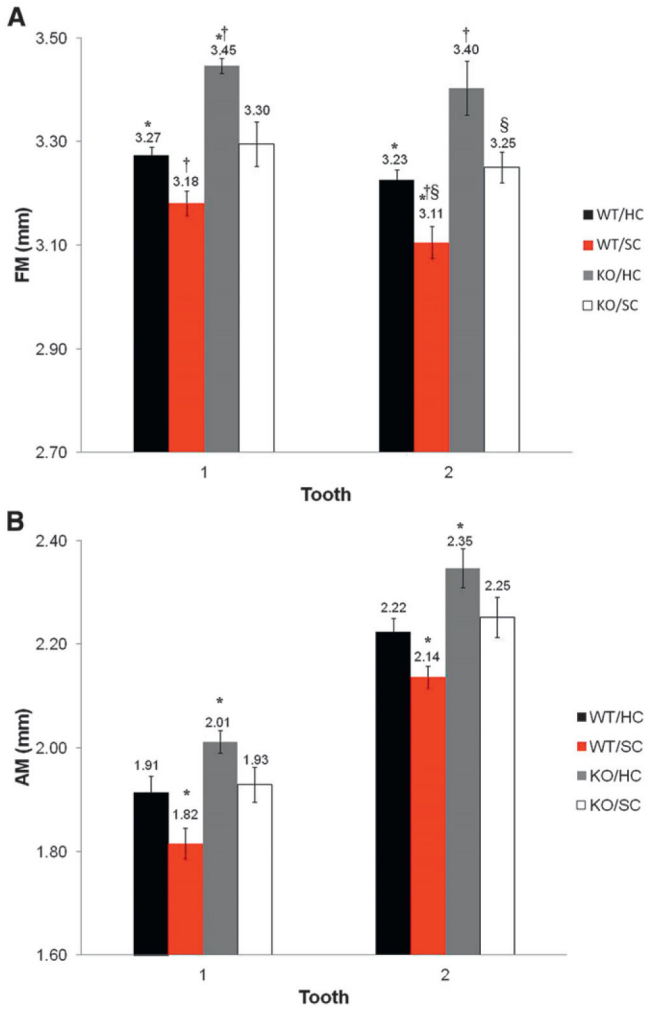

Figure 4.

The results of the comparison of the furcation positions (FM) **(A)** and the apex positions (AM) **(B)** in relation to the Pg–Gn plane among the four experimental groups at 24 weeks. Groups with the same symbols showed statistically significant differences at the given tooth ($P \leq 0.05$).

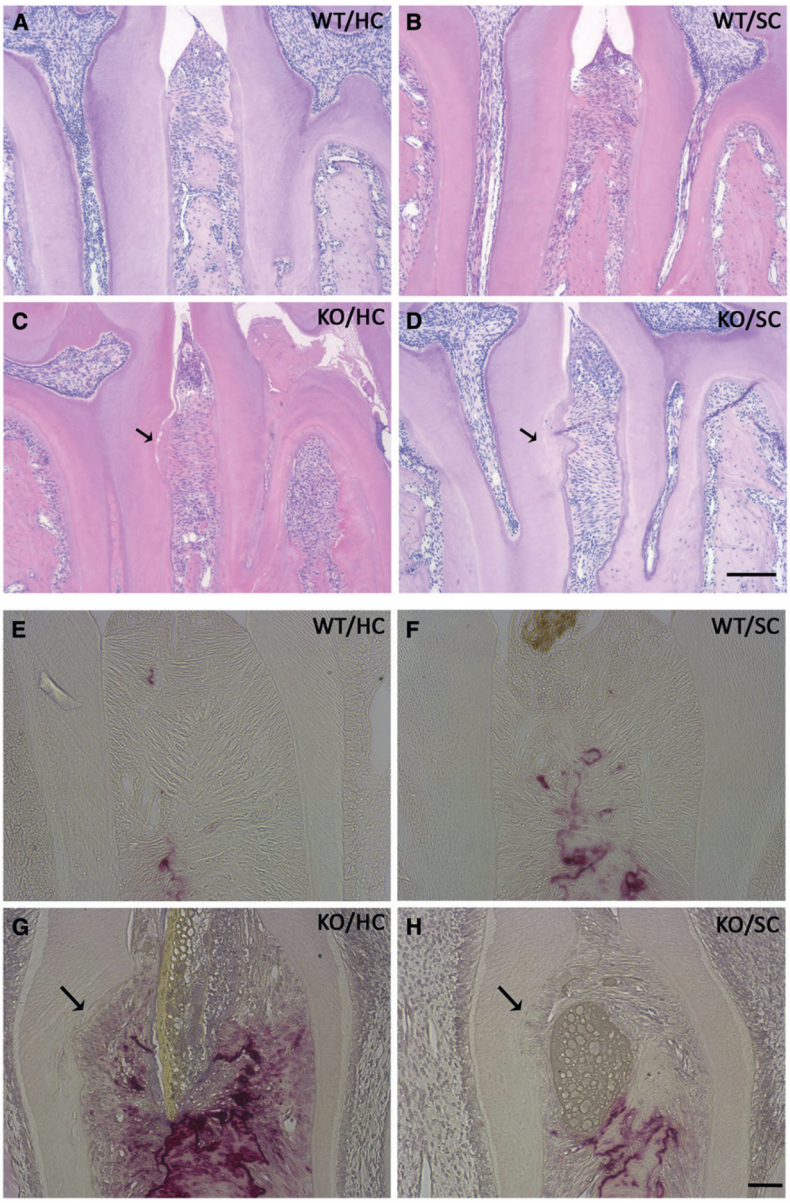

Figure 5.

A through D) Representative histologic (24-week-old mice) sections from the four experimental groups. Note significantly lowered interdental bone height, reduced interdental width, presence of a cervical root defect (black arrow), and disorganized JE in KO groups. (H&E; scale bar = 100 μm.) **E through H)** Representative immunohistologic (3-week-old mice) sections from the four experimental groups. The root defects (black arrows) in KO groups did not show TRAP staining (TRAP; scale bar = 50 μm.)